Structural Engineering and Mechanics, *Vol. 66, No. 4 (2018) 453-463*
DOI: https://doi.org/10.12989/sem.2018.66.4.453

Simulation of crack initiation and propagation in three point bending test using PFC2D

Hadi Haeri*[1], Vahab Sarfarazi[2], Zheming Zhu**[1], Ahmadreza Hedayat[3], Maryam Firoozi Nezamabadi[4] and Mohammadamin Karbala[5]

[1]*College of Architecture and Environment, Sichuan University, Chengdu 610065, China*
[2]*Department of Mining Engineering, Hamedan University of Technology, Hamedan, Iran*
[3]*Department of Civil and Environmental Engineering, Colorado School of Mines, Golden, CO 80401, United States*
[4]*Department of Civil Engineering, South Tehran Branch, Islamic Azad University, Tehran, Iran*
[5]*Department of Mining Engineering, Amirkabir University of Technology (Tehran polytechnic), Tehran, Iran*

(Received November 6, 2017, Revised February 14, 2018, Accepted February 20, 2018)

Abstract. Three points bending flexural test was modelled numerically to study the crack propagation in the pre-cracked beams. The pre-existing double internal cracks inside the beam models were considered to investigate the crack propagation and coalescence paths within the modelled samples. Notch configuration effects on the failure stress were considered too. This numerical analysis shown that the propagation of wing cracks emanating from the tips of the pre-existing internal cracks caused the final breaking of beams specimens. It was also shown that when two notches were overlapped, they both mobilized in the failure process and the failure stress was decreased when the notches were located in centre line. However, the failure stress was increased by increasing the bridge area angle. Finally, it was shown that in all cases, there were good agreements between the discrete element method results and, the other numerical and experimental results.

In this research, it is tried to improve the understanding of the crack propagation and crack coalescence phenomena in brittle materials which is of paramount importance in the stability analyses of rock and concrete structures, such as the underground openings, rock slopes and tunnel construction.

Keywords: three point bending test; beam; pre-existing double internal cracks

1. Introduction

The strength of concrete structures may be considerably reduced due to the propagation and coalescence of internal cracks under different loading conditions. The mechanical behaviour of these internal cracks within the concrete can affect the mechanism of failure and fracture of concrete structures. Therefore, the mechanism of crack propagation and control of cracking in concrete beams are generally some serious problems in the fracture mechanics designed base of engineering structures.

The Brazilian disc specimens under three and four-point bending used to perform the flexure tests in concrete beams. These experimental samples are specially prepared for determining the Mode I and Mode II fracture toughness and the tensile strength of the concrete structures. Several researches used these tests to study the fracturing mechanism of various materials under line loading condition (Dai *et al.* 2011, Wang *et al.* 2011, Wang *et al.* 2012, Yoshihara 2013, Lancaster *et al.* 2013, Jiang *et al.* 2014, Noel and Soudki 2014).

Zeng *et al.* (2014) predicted the fracture processes of asphalt mixtures by using the beam specimens under three-point bending through a damage model mechanism.

They studied the effects of crack location and the distribution of coarse aggregates on the damage behaviour and crack propagation paths of the asphalt mixtures. They also showed that these simulation results are in good agreement with their corresponding experimental results. The shear deformations in reinforced concrete beam (BRC) specimens were studied by Wang *et al.* (2015) by considering the low span-effective depth ratios. They studied a multi-angle truss model which was proposed to predict the diagonal crack angles. The bending moment variation along the span was analysed and its effects on the diagonal crack angles was also considered. Finally, their experimental results were in the good agreement with the numerical predictions of the diagonal crack angles. The cracks initiation and propagation of the pre-existing cracks in many brittle specimens and under various loading conditions have been investigated by many experimental and numerical works (Belytschko *et al.* 1999, Silling 2000, Yang *et al.* 2009, Janeiro and Einstein 2010, Yang 2011, Cheng-Zhi and Ping 2012, Ameen *et al.* 2011, Leonel *et al.* 2012, Yoshihara 2013, Lancaster *et al.* 2013, Jiang *et al.* 2014, Janeiro and Einstein 2010, Zhou *et al.* 2012, Zeng *et al.* 2014, Noel and Soudki 2014, Oliveira and Leonel 2014, Zhou *et al.* 2015, Yang 2015, Haeri 2015, Li *et al.* 2015, Li *et al.* 2016, Li *et al.* 2016, Haeri *et al.* 2016a, b, Sarfarazi *et al.* 2014, Zhou *et al.* 2015, Sarfarazi *et al.* 2016a, b, c,

*Corresponding author, Professor
E-mail: haerihadi@gmail.com
**Corresponding author, Professor
E-mail: zhemingzhu@hotmail.com

http://www.techno-press.com/journals/sem&subpage=7
ISSN: 1225-4568 (Print), 1598-6217 (Online)

Table 1 Micro properties used to represent the concrete

Parameter	Value	Parameter	Value
Type of particle	disc	Parallel bond radius multiplier	1
density	3000	Young modulus of parallel bond (GPa)	40
Minimum radius	0.27	Parallel bond stiffness ratio	1.7
Size ratio	1.56	Particle friction coefficient	0.4
Porosity ratio	0.08	Parallel bond normal strength, mean (MPa)	7
Damping coefficient	0.7	Parallel bond normal strength, SD (MPa)	2
Contact young modulus (GPa)	40	Parallel bond shear strength, mean (MPa)	7
Stiffness ratio	1.7	Parallel bond shear strength, SD (MPa)	2

(a)

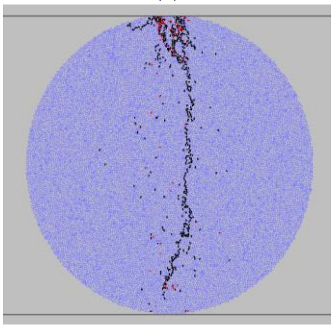

(b)

Fig. 2 failure pattern in (a) physical sample, (b) PFC2D model

Sarfarazi and Haeri *et al.* 2016, Sardemir 2016, Shuraim 2016, Shaowei *et al*. 2016, Bi *et al.* 2016, Zhou *et al.* 2016, Wang *et al.* 2017, Silling 2017, Bi *et al.* 2017).

However, in this study, the crack propagation mechanism of concrete specimens is investigated by simulating some flexural tests through a discrete element approach using a sophisticated particle flow code (PFC2D)). The crack initiation and propagation of the pre-existing double internal cracks is investigated by simulating the four points bending test. The effects of cracks inclination angles and cracks configurations on the specimens fracturing path with in the bridge areas of the samples are studied by this numerical simulation procedure. These numerical fracturing patterns are compared with the corresponding experimental results showing that they are well fitted with experimentally obtained patterns.

2. Particle flow code (PFC2D)

The mechanical behaviour of a material can be

Table 2 Brazilian tensile strength of physical and numerical samples

Physical tensile strength (MPa)	1.5 and 1.7
Numerical tensile strength (MPa)	1.5

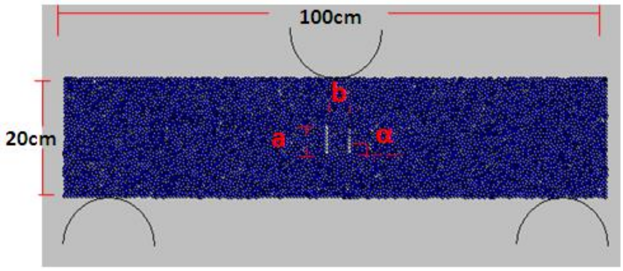

Fig. 3 The PFC specimen under three point bending test

simulated by the particle flow code (PFC2D) by representing it as an assembly of circular particles that can be bonded to one another. The discrete element approach within the PFC2D (as described by Cundall and Strack 1979) can model the movement and interaction of the particles within a particular material sample.

It should be noted that, the DEM was originally applied to simulate the behaviour of granular materials. Then, by introducing the ability to bond together the adjacent particles using the parallel or/and contact bonds, the procedure has been extended and applied to simulate the more complex problems in solid mechanics. A concrete beam specimen can be modelled by considering a rectangular assembly of particles with specified statistical size distributions which are bounded together with four rigid walls. An automatic particle generator (with their radii being distributed either uniformly or according to a Gaussian distribution) is established in the computer code to generate these particles. Then, the bonds are installed into the neighbouring particles so that the overall mechanical behaviour of the assembly is dominated by the micro-properties of these particles and bonds. It was already described in detail by Potyondy and Cundall, in 2003 that the standard process of generating bonding particles assemblies to represent a biaxial test model of a cylindrical concrete sample involves the following five important steps: i) particle generation, ii) packing of the particles, iii) isotropic stress installation (stress initialization with in the particles), iv) floating particle (floater) eliminations and v) bonding installation (the parallel bond is a better bond for cementations material like concrete).

2.1 Preparing and calibrating the numerical model

The Brazilian test was used to calibrate the tensile strength of specimen in PFC2D model (Ghazvinian *et al.* 2012). Adopting the micro-properties listed in Table 1 and the standard calibration procedures (Potyondy and Cundall 2003), a calibrated PFC particle assembly was created. The diameter of the Brazilian disk considered in the numerical tests was 54 mm. The specimen was made of 5,615 particles. The disk was crushed by the lateral walls moved toward each other with a low speed of 0.016 m/s. Figs. 2(a),

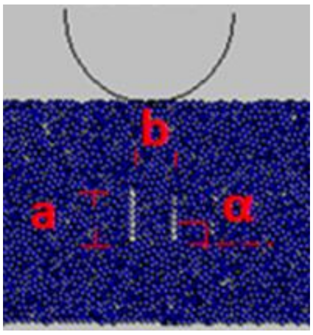

(a)

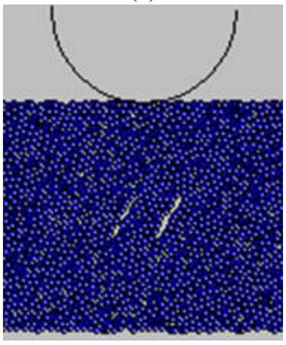

(b)

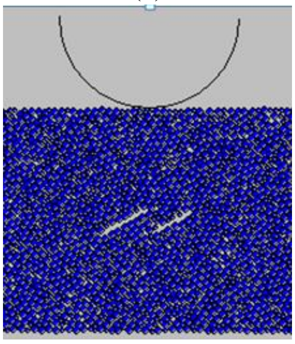

(c)

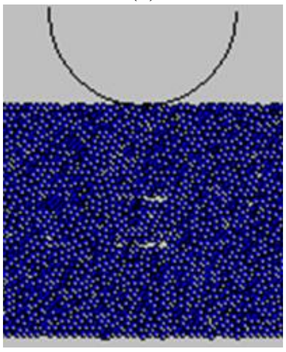

(d)

Fig. 4 Different types of models with notch angularities of; (a) 90°, (b) 60°, (c) 30° and (d) 0°

(b) illustrate the failure patterns of the numerical and experimental tested samples, respectively. The failure planes experienced in numerical and laboratory tests are well matching. The numerical tensile strength and a comparison of its experimental measurements were presented in Table 2. This table shows a good accordance between numerical and experimental results. The numerical and experimental load-displacement curves in Brazilian

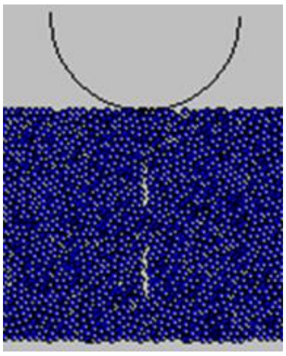

(a)

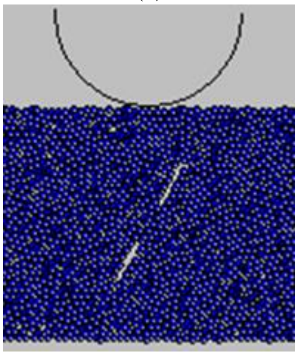

(b)

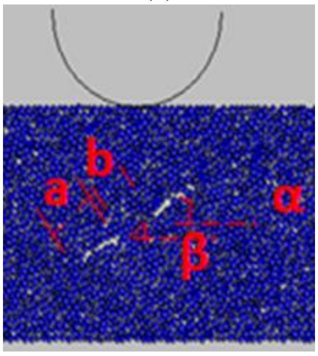

(c)

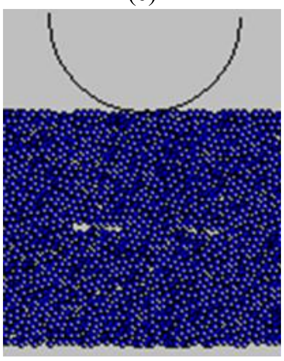

(d)

Fig. 5 Different types of models with notch angularities (α)-bridge area angularities(β) of; (a) 90°-90°, (b) 60°-60°, (c) 30°-30° and (d) 0°-0°

samples have been shown in Ghazvinian *et al.* (2012).

2.2 Model preparation using particle flow code

After calibration of PFC2D, three point flexural tensile

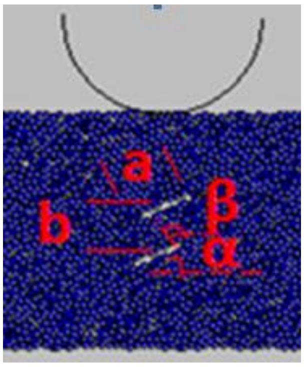

(a)

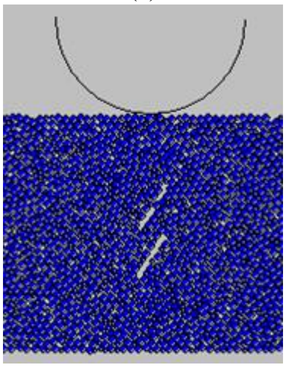

(b)

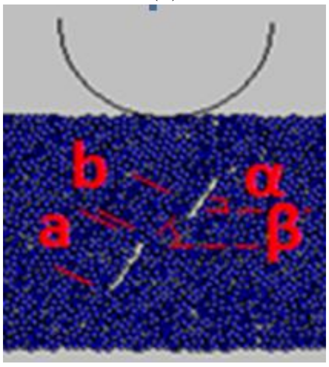

(c)

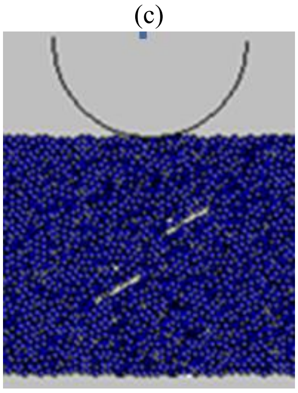

(d)

Fig. 6 Different types of models with notch angularities (α)-bridge area angularities(β) of; (a) 30°-145°, (b) 60°-165°, (c) 60°-30° and (d) 30°-60°

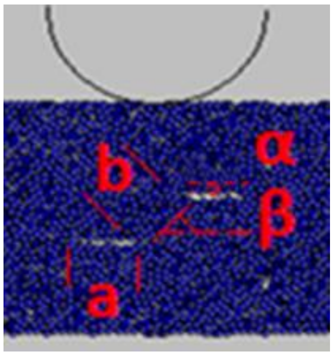

(a)

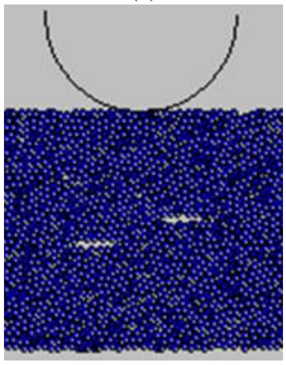

(b)

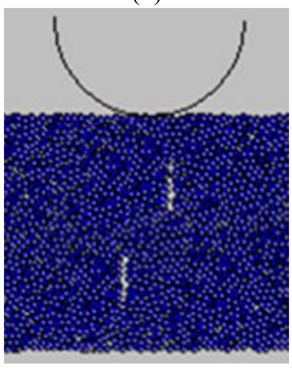

(c)

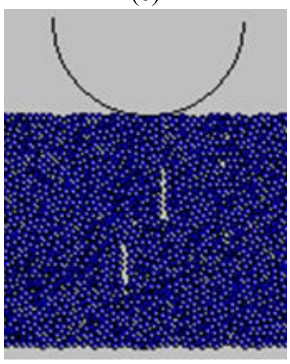

(d)

Fig. 7 Different types of models with notch angularities (α)-bridge area angularities(β) of; a) 0°-60°, b) 0°-30°, (c) 90°-60° and d) 90°-30°

tests were simulated by creating a beam model in PFC2D (by using the calibrated micro-parameters) (Fig. 3). The PFC specimen had dimension of 20 cm×100 cm. A total of 7,179 disks with a minimum radius of 0.27 mm were used to prepare the beam model. These models contain two parallel centred cracks. These notches have various configurations in the models (Figs. 4-7).

The first set of models have two parallel notch situated in horizontal centreline (Fig. 4). The notch lengths (a) were

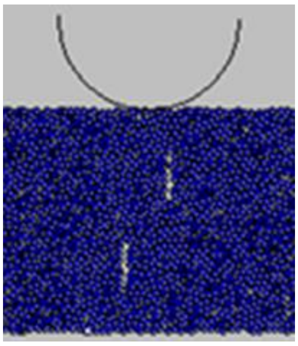

(a)

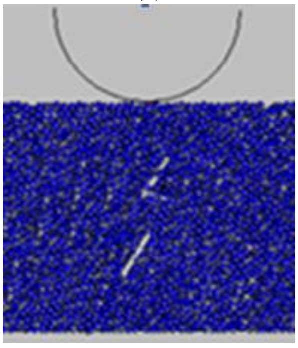

(b)

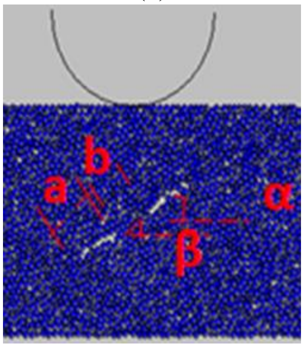

(c)

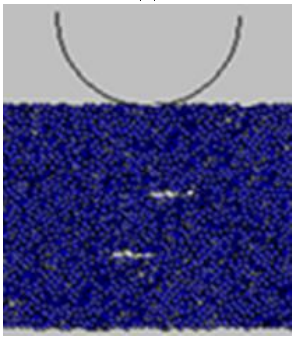

(d)

Fig. 8 Different types of models with notch angularities (α)-bridge area angularities(β) of; (a) 90°-60°, (b) 60°-90°, (c) 30°-30° and (d) 0°-90°

2 cm. The bridge length (b) was 2 cm, i.e., distance between internal tips of two joins. The angularities of joints related to horizontal line were 90°, 60°, 30° and 0°, respectively.

The second set of models have two linear non-persistent notch situated in middle of the model (Fig. 5). The notch lengths (a) were 2 cm. The bridge length (bridge area) (b) was 2 cm, i.e., distance between internal tips of two pre-

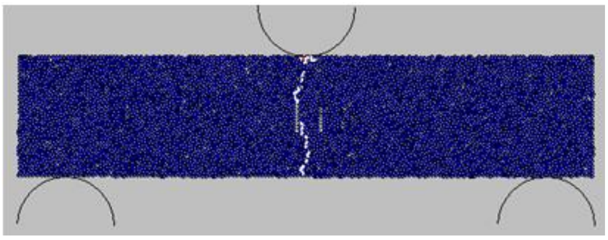

(a)

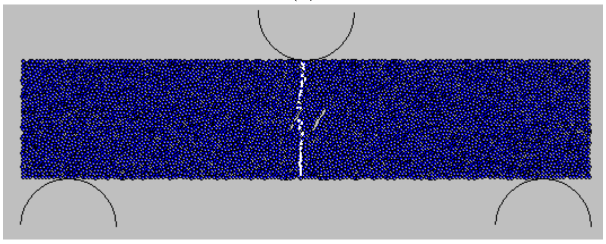

(b)

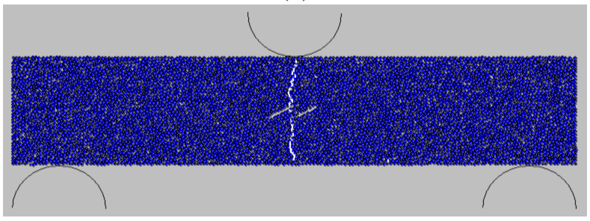

(c)

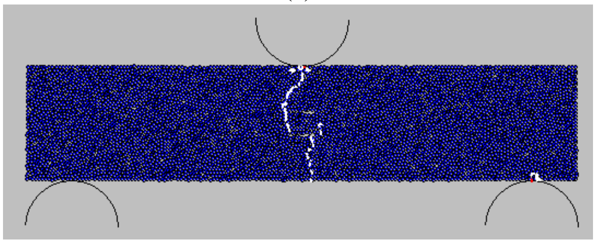

(d)

Fig. 9 Different types of cracked models with notch angularities of; (a) 90°, (b) 60°, (c) 30° and (d) 0°

existing cracks. The angularity of cracks and bridge area related to horizontal line were 90°-90°, 60°-60°, 30°-30° and 0°-0°, respectively.

The third sets of models have two oblique echelon notch situated in middle of the model (Fig. 6). The notch lengths (a) were 2 cm. The bridge length (b) was 2 cm. The angularity of cracks and bridge area related to horizontal line were 30°-145° (Fig. 6(a)), 60°-165° (Fig. 6(b)), 60°-30° (Fig. 6(c)) and 30°-60° (Fig. 6(d)), respectively.

The fourth sets of models have two echelon notch situated in middle of the model (Fig. 7). For creation of the notches, firstly clump particle is set into the model, then these clump is deleted from the model. The notch lengths (a) were 2 cm. The bridge length (b) was 2 cm. The angularity of cracks and bridge area related to horizontal line were 90°-60° (Fig. 7(a)), 90°-30° (Fig. 7(b)), 0°-60° (Fig. 7(c)) and 0°-30° (Fig. 7(d)), respectively.

This flaw geometry is different from those reported in the previous studies, where only one flaw was used. The beam was crushed by two lower circle walls moved upward and one upper circle wall moved downward with a low speed of 0.016 m/s. The failure force and crack initiation force were registered by taking the reaction forces on the loading wall.

Concurrent with simulation of these models, four different models with different configuration similar to models tested by Haeri *et al.* (2016) were prepared, i.e., two vertical cracks; crack angle and bridge area angle are 90° and 60° (Fig. 8(a)), (b) two inclined cracks; crack angle and bridge area angle are 60° and 90° (Fig. 8(b)), (c) two parallel inclined cracks; crack angle and bridge area angle are 30° and 30° (Fig. 8(c)), (d) two horizontal cracks; joint angle and bridge area angle are 0° and 90° (Fig. 8(d)).

3. Failure behaviour of numerical models

3.1 Failure mechanism of model consisting of two surrounded notches

a) Failure mechanism in models with two parallel notches
When two parallel notches exist in the model (Fig. 9(a)), tensile crack initiates from lower edge of the model and propagates vertically till coalesce with lower tip of the left notch. A similar tensile crack initiates from upper tip of the left notch and propagates vertically till coalesce with upper edge of the model.

For cracks oriented at 60° (Fig. 9(b)), a tensile crack initiates from lower edge of the model and propagates vertically till coalesce with middle of the left notch. Similarly, another tensile crack initiates from upper tip of the left notch and propagates vertically till coalesce with upper edge of the model.

For cracks with a 30° orientation (Fig. 9(c)), tensile cracks initiate first from the lower edge of the model and then from the upper tip of the left notch and propagate until they coalesce with the outer edges of the specimen.

In the beam specimen with horizontal cracks (Fig. 9(d)), a tensile crack initiates from lower edge of the model and propagates vertically till coalesce with right tip of the lower notch. Another tensile crack initiates from left tip of the lower notch and propagates vertically and coalesces with left tip of upper notch. This crack propagate parallel to loading axis till coalesce with upper edge of the model.

b) Failure mechanism in models with two linear non-persistent cracks

When two non-persistent notches exist in the model (Fig. 10(a)), a tensile crack initiates from lower edge of the model and propagates vertically till it coalesces with lower tip of the lower notch. Another tensile crack initiates from upper tip of the lower notch and propagates parallel to loading axis until it coalesces with lower tip of the upper joint. This crack grows until it reaches the upper edge of the specimen. For notches oriented at 60° (Fig. 10(b)), the first tensile crack initiates from lower edge of the model and propagates vertically till coalesce with middle of the left notch. The second tensile crack initiates from upper tip of the left notch and propagates diagonally till coalesce with lower tip of the right notch. The third tensile crack initiates from upper tip of the right notch and propagates vertically till it reaches the specimen edge. For the specimen with notches oriented at 30° (Fig. 10(c)), a tensile crack initiates

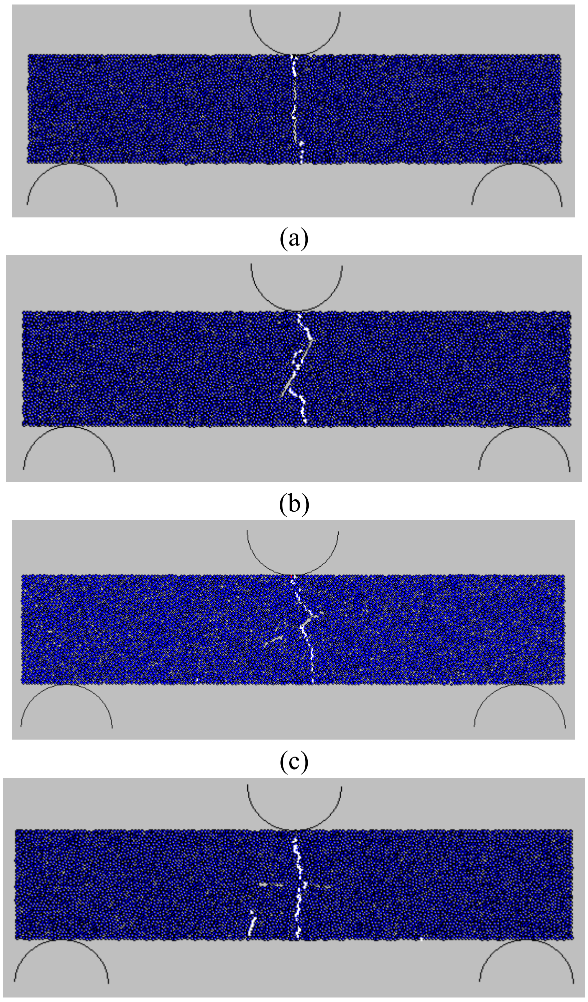

(a)

(b)

(c)

(d)

Fig. 10 Different types of cracked models with notch angularities (α)-bridge angularities(β) of; (a) 90°-90°, (b) 60°-60°, (c) 30°-30° and (d) 0°-0°

from lower edge of the model and propagates vertically till coalesce with lower tip of the right notch. Another tensile crack initiates from upper tip of the right notch and propagates vertically till it coalesces with upper edge of the model. When two non-persistent horizontal notches exist in the model (Fig. 10(d)), a tensile crack initiates from lower edge of the model and propagates vertically till coalesce with left tip of the right notch. Another tensile crack initiates from this place and propagates vertically till it reaches the upper edge of the specimen.

c) Failure mechanism in models with two oblique echelon notches

When the joint angle and the bridge area angle are 30° and 145°, respectively (Fig. 11(a)), a tensile crack initiates first from the lower edge of the model and approaches the tip of the upper notch. Another tensile crack initiates from this point and grows until it reaches the upper edge of the model. When joint angle and bridge area angle are 60° and 30°, respectively (Fig. 11(b)), the first tensile crack initiates from lower edge of the model and propagates vertically till it coalesces with lower tip of the upper notch. The second tensile crack initiates from this point and propagates

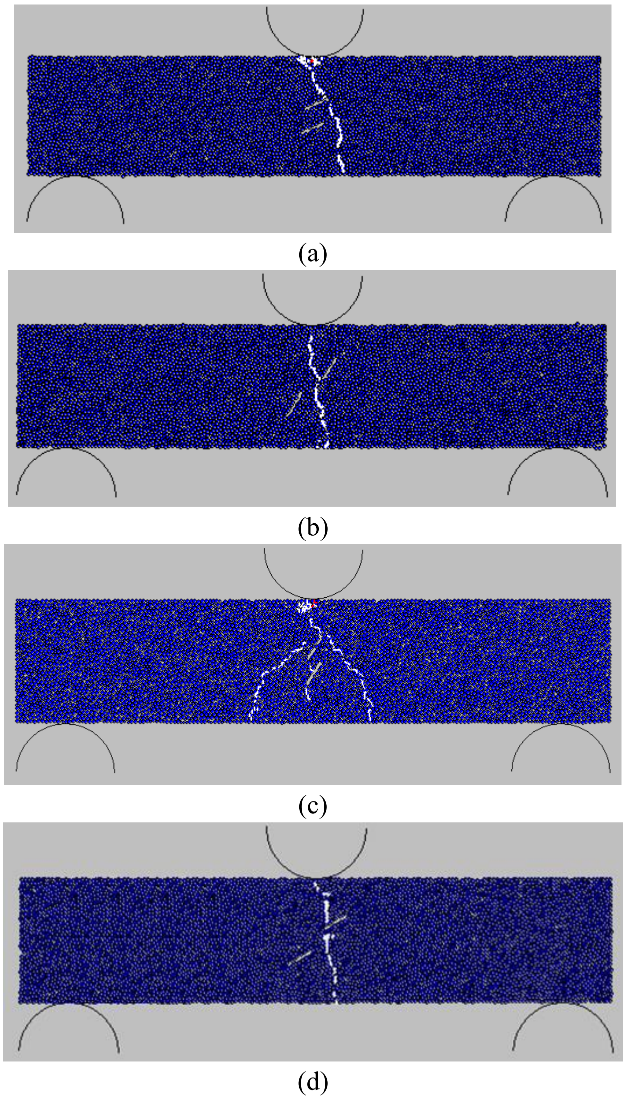

Fig. 11 Different types of cracked models with notch angularities (α)-bridge angularities(θ) of; (a) 30°-145°, (b) 60°-30°, (c) 60°-165° and (d) 30°-60°

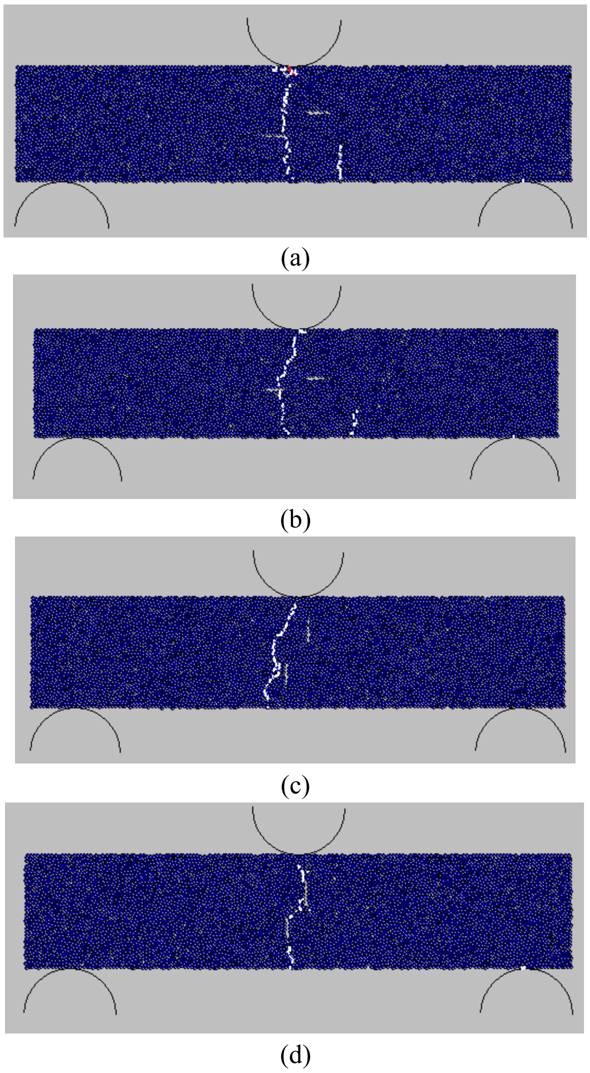

Fig. 12 Different types of cracked models with notch angularities (α)-bridge angularities(β) of; (a) 0°-60°, (b) 0°-30°, (c) 90°-60° and (d) 90°-30°

vertically until it coalesces with the upper edge.

When joint angle and bridge area angle are 60° and 165°, respectively (Fig. 11(c)), tensile cracks initiate from two points on the lower edge of the model and propagate diagonally till they reach the upper tip of the upper notch. Another tensile crack initiates from the upper tip of the upper notch and propagates vertically till it coalesces with the upper edge of the model. When joint angle and bridge area angle are 30° and 60°, respectively (Fig. 11(d)), a tensile crack initiates from lower edge of the model and propagates vertically till it coalesces with left tip of the right notch. Another tensile crack initiates from this place and propagates vertically till it coalesces with upper edge of the model.

d) Failure mechanism in models with two echelon notches

When joint angle and bridge area angle are 0° and 60°, respectively (Fig. 12(a)), tensile crack initiates from lower edge of the model and propagates vertically till coalesce with right tip of the lower notch. Another tensile crack initiates from this place and propagates parallel to loading axis till coalesce with edge of the model.

When joint angle and bridge area angle are 0° and 30°, respectively (Fig. 12(b)), first set of tensile crack initiates from lower edge of the model and propagates vertically till coalesce with lower tip of the lower notch. Second set of tensile crack initiates from upper tip of the lower notch and propagates diagonally till coalesce with lower tip of the upper notch. Third set of tensile crack initiates from upper tip of the upper joint and propagates vertically till coalesce with edge of the model. When joint angle and bridge area angle are 90° and 60°, respectively (Fig. 12(c)), tensile crack initiates from lower edge of the model and propagates nearly vertically till coalesce with upper edge of the model. In this condition none of the notches mobilized in failure process. When joint angle and bridge area angle are 90° and 30°, respectively (Fig. 12(d)), tensile crack initiates from lower edge of the model and propagates vertically till coalesce with right tip of the lower notch. Another tensile crack initiates from this place and propagates vertically till coalesce with upper edge of the model.

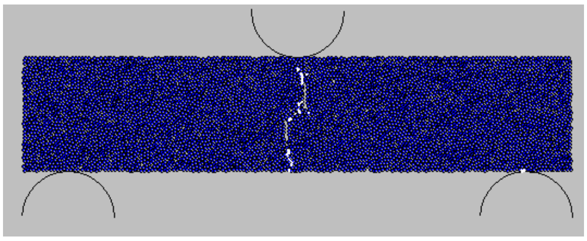

(a)

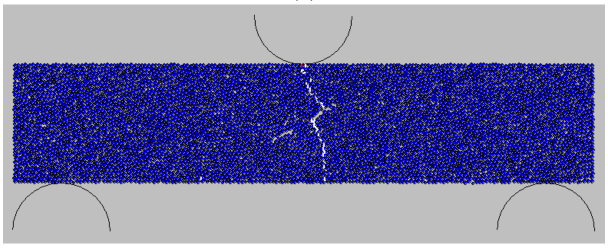

(b)

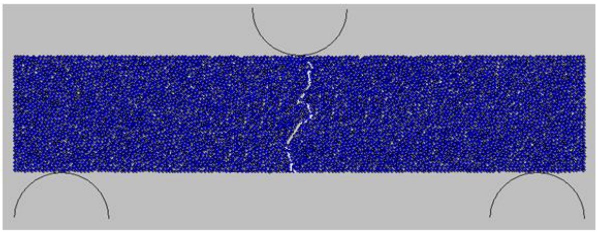

(c)

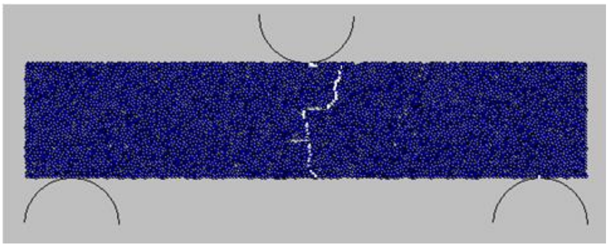

(d)

Fig. 13 Different types of cracked models with notch angularities (α)- bridge angularities(β) of; (a) 0°-60°, (b) 30°-30°, (c) 60°-90° and (d) 90°-90°

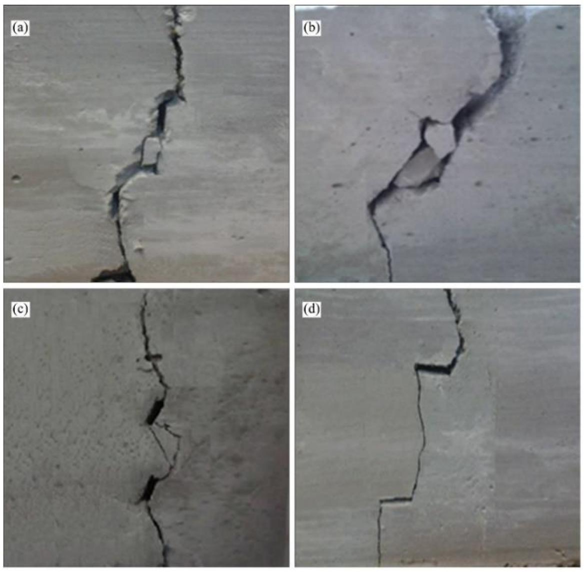

Fig. 14 Cracking patterns in double cracked beam specimens containing different crack positions: (a) Two vertical cracks; (b) Two inclined cracks; (c) Two parallel inclined cracks; (d) Two horizontal cracks (Haeri *et al.* 2015)

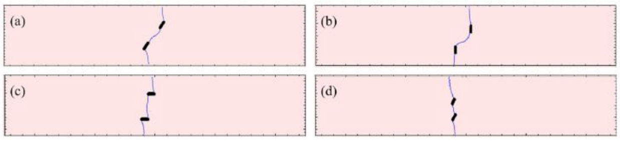

Fig. 15 Numerical simulation of crack propagation paths and cracks coalescence for double cracked beam specimens under three-point bending: (a) Two vertical cracks; (b) Two inclined cracks; (c) Two parallel inclined cracks; (d) Two horizontal cracks (Haeri *et al.* 2015)

e) Failure mechanism in models with different notch configurations

When joint angle and bridge area angle are 0° and 60°, respectively (Fig. 13(a)), first set of tensile crack initiates from lower edge of the model and propagates vertically till coalesce with lower tip of the lower notch. Second set of tensile crack initiates from upper tip of the lower notch and propagates diagonally till coalesce with lower tip of the upper notch. Third set of tensile crack initiates from upper tip of the upper joint and propagates vertically till coalesce with edge of the model.

When the angularity of non-persistent notches and bridge area related to horizontal line were 30° (Fig. 13(b)), tensile crack initiates from lower edge of the model and propagates vertically till coalesce with lower tip of the right notch. Another tensile crack initiates from upper tip of the right notch and propagates vertically till coalesce with upper edge of the model.

When joint angle and bridge area angle are 60° and 90°, respectively (Fig. 13(c)), first set of tensile crack initiates from lower edge of the model and propagates vertically till coalesce with lower tip of the lower notch. Second set of tensile crack initiates from upper tip of the lower notch and propagates diagonally till coalesce with lower tip of the upper notch. Third set of tensile crack initiates from upper tip of the upper joint and propagates vertically till coalesce with edge of the model.

When joint angle and bridge area angle are 90° and 90°, respectively (Fig. 13(d)), the first set of tensile crack initiates from lower edge of the model and propagates vertically till coalesces with the right tip of the lower notch. The second tensile crack initiates from this place and propagates vertically till coalesce with left tip of the upper joint. The third set of tensile cracks initiate from right side of upper notch and propagates vertically till coalesce with edge of the model.

Totally, the results show that when two notches are overlapped, nearly two notches mobilized in failure process. Also, the failure stress is decreased when notches exist in centre line. The failure stress is increased by increasing the bridge area angle.

As can be observed by comparing between Figs. 13 and 14, there is good accordance between numerical simulation and experimental results obtained by Haeri *et al.* (2015).

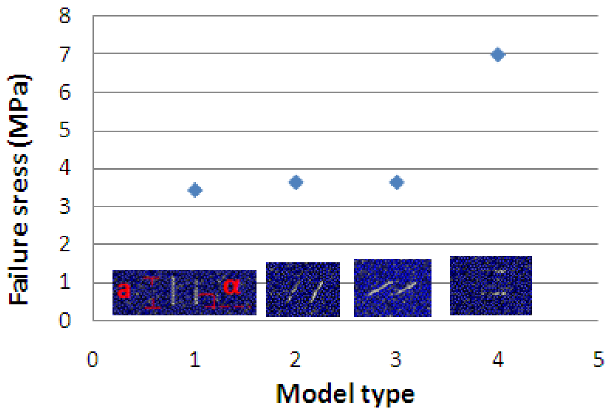

(a)

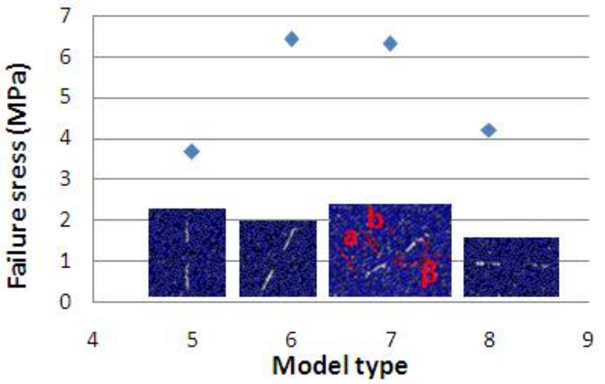

(b)

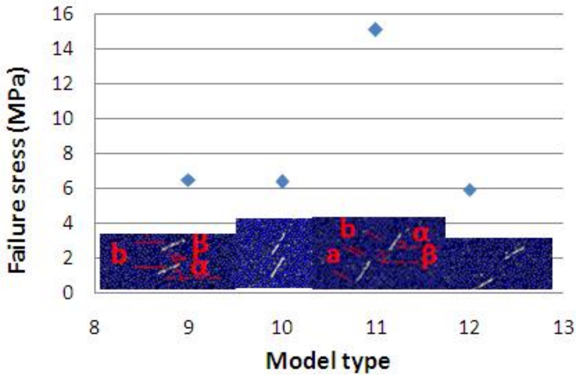

(c)

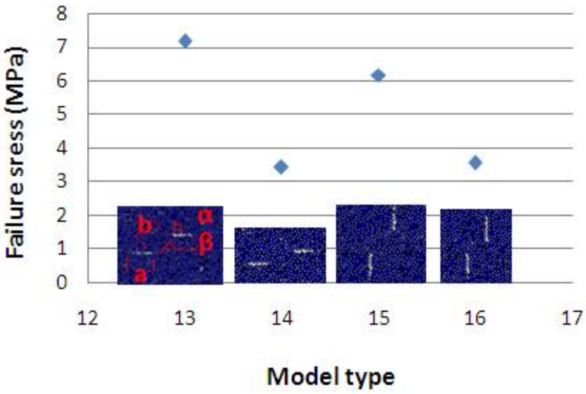

(d)

Fig. 16 variation of failure stress versus notch configuration

Haeri *et al.* (2015) simulated numerically the crack propagation in beam models with same notch configuration. Comparison between Figs. 13 and 15, shows that the simulated propagation paths are in good agreement with the corresponding high order DDM numerical results obtained by Haeri *et al*. (2015).

3.2 The effect of notch configuration on the failure stress

Fig. 16 shows the effect of notch configuration on the failure stresses. Failure stress (σ) was measured based on maximum momentum on the beam (M), maximum distance from neutral line (c) and momentum inertia (I), i.e., $\sigma = \frac{Mc}{I}$. As can be seen from Fig. 1(a), when two notches exist vertically in middle of model, failure stress has minimum value, i.e., 3.4 MPa. Fig. 3(b) shows that model number 5 with two linear vertical notches has minimum failure stress, i.e., 3.6 MPa. Fig. 3(c) shows that model number 12 with two linear vertical notches has minimum failure stress, i.e., 6 MPa. Fig. 3(d) shows that model number 12 with two linear vertical notches has minimum failure stress, i.e., 3.5 MPa. Totally, it can be concluded that model number 1 with two vertical notches has minimum tensile strength.

4. Conclusions

A discrete element approach simulating the four point bending concrete specimens has been proposed to study the mechanism of crack propagation in concrete beam specimens. In this approach, each specimen contains two pre-existing internal cracks specially prepared within the modelled samples. Then, various types of these specially prepared double cracked beam specimens are numerically tested by using a two-dimensional particle flow code. These numerical analyses results well illustrate that the cracks propagation paths can be produced by the coalescence phenomenon of the pre-existing internal cracks in these tests. However, it has been shown that the fracturing of double cracked specimens occurs mainly by the propagation of wing cracks emanating from the tips of the two pre-existing internal cracks. These results also showed that when the two notches were overlapped, they mobilized in failure process. Also, the failure stress was decreased when these notches were located in centre line of the modelled samples. The failure stress was also increased by increasing the bridge area angle with in the simulated test samples.

It has been shown that there is a good agreement between the discrete element simulating results obtained in this research and the other numerical and experimental results cited in the literature.

It's to be note that the limitations of DEM are (Donze *et al.* 2009): (a) Fracture is closely related to the size of elements, and that is so called size effect. (b) Cross effect exists because of the difference between the size and shape of elements with real grains. (c) In order to establish the relationship between the local and macroscopic constitutive laws, data obtained from classical geomechanical tests which may be impractical are used.

References

Ameen, M., Raghu Prasad, B.K. and Gopalakrishnan, A.R. (2011), "Modeling of concrete cracking-a hybrid technique of using displacement discontinuity element method and direct boundary element method", *Eng. Analy. Bound. Elem.*, **35**(9), 1054-1059.

Belytschko, T. and Black, T. (1999), "Elastic crack growth in finite elements with minimal remeshing", *Int. J. Numer. Meth. Eng.*, **45**(5), 601-620.

Bi, J., Zhou, X.P. and Qian, Q.H. (2016), "The 3D Numerical simulation for the propagation process of multiple pre-existing flaws in rock-like materials subjected to biaxial compressive loads", *Rock Mech. Rock Eng.*, **49**(5), 1611-1627.

Bi, J., Zhou, X.P. and Xu, X.M. (2017), "Numerical simulation of failure process of rock-like materials subjected to impact loads", *Int. J. Geomech.*, **17**(3), 04016073

Bobet, A. (2000), "The initiation of secondary cracks in compression", *Eng. Fract. Mech.*, **66**(2), 187-219.

Bombolakis, E.G. (1968), "Photoelastic study of initial stages of brittle fracture in compression", *Tectonophys.*, **6**(6), 461-473.

Cundall, P.A. and Strack, O.D.L. (1979), "A discrete numerical model for granular assemblies", *Geotech.*, **29**(1), 47-65.

Donze, F.V., Richefeu, V. and Magnier, S.A. (2009), "Advances in discrete element method applied to soil rock and concrete mechanics", *Electr. J. Geol. Eng.*, **8**(1), 1-44.

Erdogan, F. and Sih, G.C. (1963), "On the crack extension path in plates under plane loading and transverse shear", *ASME J. Bas. Eng.*, **85**(4), 519-527.

Ghazvinian, A., Sarfarazi, V., Schubert, W. and Blumel, M. (2012), "A study of the failure mechanism of planar non-persistent open joints using PFC2D", *Rock Mech. Rock Eng.*, **45**(5), 677-693.

Haeri, H. (2015), "Influence of the inclined edge notches on the shear-fracture behavior in edge-notched beam specimens", *Comput. Concrete*, **16**(4), 605-623.

Haeri, H. (2016), "Propagation mechanism of neighboring cracks in rock-like cylindrical specimens under uniaxial compression", *J. Min. Sci.*, **51**(5), 1062-1106.

Haeri, H., Khaloo, A. and Marji, M.F. (2015), "Experimental and numerical simulation of the microcrack coalescence mechanism in rock-like materials", *Strength Mater.*, **47**(5), 740-754.

Haeri, H., Sarfarazi, V. and Hedayat, A. (2016a), "Suggesting a new testing device for determination of tensile strength of concrete", *Struct. Eng. Mech.*, **60**(6), 939-952.

Haeri, H., Sarfarazi, V. and Lazemi, H. (2016b), "Experimental study of shear behavior of planar non-persistent joint", *Comput. Concrete*, **17**(5), 639-653.

Haeri, H., Shahriar, K. and Marji, M.F. (2013), "Modeling the propagation mechanism of two random micro cracks in rock samples under uniform tensile loading,", *Proceedings of the ICF13*.

Hoek, E. and Bieniawski, Z.T. (1965), "Brittle fracture propagation in rock under compression", *Int. J. Fract.*, **1**(3), 137-155.

Hussian, M.A., Pu, E.L. and Underwood, J.H. (1974), *Strain Energy Release Rate for a Crack under Combined Mode I and Mode II. In: Fracture Analysis*, ASTM STP 560, American Society for Testing and Materials, 2-28.

Ingraffea, A.R. and Heuze, F.E. (1980), "Finite element models for rock fracture mechanics", *Int. J. Numer. Analy. Meth. Geomech.*, **4**(1), 25-43.

Itasca, C.G. (2002), *Users' Manual for Particle Flow Code in 2 Dimensions (PFC2D)*, Version 3.1, Minneapolis, Minnesota, U.S.A.

Janeiro, R.P. and Einstein, H.H. (2010), "Experimental study of the cracking behavior of specimens containing inclusions (under uniaxial compression)", *Int. J. Fract.*, **164**(1), 83-102.

Jiang, Z., Wan, S., Zhong, Z., Li, M. and Shen, K. (2014), "Determination of mode-I fracture toughness and non-uniformity for GFRP double cantilever beam specimens with an adhesive layer", *Eng. Fract. Mech.*, **128**, 139-156.

Jiefan, H., Ganglin, C., Yonghong, Z. and Ren, W. (1990), "An experimental study of the strain field development prior to failure of a marble plate under compression", *Tectonophys.*, **175**(1-3), 184-269.

Lajtai, E.Z. (1971), "A theoretical and experimental evaluation of the Griffith theory of brittle fracture", *Tectonophys.*, **11**(2), 129-156.

Lajtai, E.Z. (1974), "Brittle fractures in compression", *Int. J. Fract.*, **10**(4), 525-536.

Lancaster, I.M., Khalid, H.A. and Kougioumtzoglou, I.A. (2013), "Extended FEM modelling of crack propagation using the semi-circular bending test", *Constr. Build. Mater.*, **48**, 270-277.

Leonel, E.D., Chateauneuf, A. and Venturini, W.S. (2012), "Probabilistic crack growth analyses using a boundary element model: Applications in linear elastic fracture and fatigue problems", *Eng. Analy. Bound. Elem.*, **36**, 944-959.

Li, Y.P., Chen, L.Z. and Wang, Y.H. (2005), "Experimental research on pre-cracked marble under compression", *Int. J. Sol. Struct.*, **42**, 2505-2516.

Miller, J.T. and Einstein, H.H. (2008), "Crack coalescence tests on granite", *Proceedings of the 42nd US Rock Mechanics Symposium*, San Francisco, U.S.A.

Mughieda, O. and Alzoubi, A.K. (2004), "Fracture mechanisms of offset rock joints-a laboratory investigation", *Geotech. Geol. Eng.*, **22**(4), 545-562.

Noel, M. and Soudki, K. (2014), "Estimation of the crack width and deformation of FRP-reinforced concrete flexural members with and without transverse shear reinforcement", *Eng. Struct.*, **59**, 393-398.

Oliveira, H.L. and Leonel, E.D. (2014), "An alternative BEM formulation, based on dipoles of stresses and tangent operator technique, applied to cohesive crack growth modeling", *Eng. Analy. Bound. Elem.*, **41**, 74-82.

Ozecebe, G. (2011), "Minimum flexural reinforcement for T-beams made of higher strength concrete", *Can. J. Civil Eng.*, **26**(5), 525-534.

Park, N.S. (2001), "Crack propagation and coalescence in rock under uniaxial compression", M.Sc. Dissertation, Seoul National University, Korea.

Potyondy, D.O. and Cundall, P.A. (2004), "A bonded-particle model for rock", *Int. J. Rock Mech. Min. Sci.*, **41**, 1329-1364.

Reyes, O. and Einstein, H.H. (1991), "Failure mechanisms of fractured rock-a fracture coalescence model", *Proceedings of the 7th Congress of the ISRM*, Aachen, Germany.

Ruiz, G. and Carmona, R.J. (2006a), "Experimental study on the influence of the shape of the cross-section and the rebar arrangement on the fracture of LRC beams", *Mater. Struct.*, **39**(3), 343-352.

Ruiz, G., Carmona, R.J. and Cendon, D.A. (2006b), "Propagation of a cohesive crack through adherent reinforcement layers", *Comput. Meth. Appl. Mech. Eng.*, **195**(52), 7237-7248.

Sagong, M. and Bobet, A. (2002), "Coalescence of multiple flaws in a rock-model material in uniaxial compression", *Int. J. Rock Mech. Min. Sci.*, **39**(2), 229-241.

Sardemir, M. (2016), "Empirical modeling of flexural and splitting tensile strengths of concrete containing fly ash by GEP", *Comput. Concrete*, **17**(4), 489-498.

Sarfarazi, V. and Haeri, H. (2016), "Effect of number and configuration of bridges on shear properties of sliding surface", *J. Min. Sci.*, **52**(2), 245-257.

Sarfarazi, V. and Haeri, H. (2016c), "A review of experimental and numerical investigations about crack propagation", *Comput. Concrete*, **18**(2), 235-266.

Sarfarazi, V. and Shubert, W. (2016b), “Numerical simulation of tensile failure of concrete in direct, flexural, double punch tensile and ring tests”, *Period. Polyech. Civil Eng.*, **2**, 1-8.

Sarfarazi, V., Faridi, H.R., Haeri, H. and Schubert, W. (2016c), “A new approach for measurement of anisotropic tensile strength of concrete”, *Adv. Concrete Constr.*, **3**(4), 269-284.

Sarfarazi, V., Ghazvinian, A., Schubert, W., Blumel, M. and Nejati, H.R. (2014), “Numerical simulation of the process of fracture of echelon rock joints”, *Rock Mech. Rock Eng.*, **47**(4), 1355-1371.

Sarfarazi, V., Haeri, H. and Khaloo, A. (2016a), “The effect of non-persistent joints on sliding direction of rock slopes”, *Comput. Concrete*, **17**(6), 723-737.

Shaowei, H., Aiqing, X., Xin, H. and Yangyang, Y. (2016), “Study on fracture characteristics of reinforced concrete wedge splitting tests”, *Comput. Concrete*, **18**(3), 337-354.

Shen, B. (1995), “The mechanism of fracture coalescence in compression-experimental study and numerical simulation”, *Eng. Fract. Mech.*, **51**(1), 73-85.

Shen, B. and Stephansson, O. (1994), “Modification of the G-criterion for crack propagation subjected to compression”, *Eng. Fract. Mech.*, **47**(2), 177-189.

Shuraim, A.B., Aslam, F., Hussain, R. and Alhozaimy, A. (2016), “Analysis of punching shear in high strength RC panels-experiments, comparison with codes and FEM results”, *Comput. Concrete*, **17**(6), 739-760.

Sih, G.C. (1974), “Strain-energy-density factor applied to mixed mode crack problems”, *Int. J. Fract.*, **10**(3), 305-321.

Silling, S.A. (2000), “Reformulation of elasticity theory for discontinuities and long-range forces”, *J. Phys. Sol.*, **48**(1), 175-209.

Silling, S.A. (2017), “Stability of peridynamic correspondence material models and their particle discretizations”, *Comput. Meth. Appl. Mech. Eng.*, **322**, 42-57.

Tang, C.A. and Kou, S.Q. (1998), “Crack propagation and coalescence in brittle materials under compression”, *Eng. Fract. Mech.*, **61**(3-4), 311-324.

Tang, C.A., Lin, P., Wong, R.H.C. and Chau, K.T. (2001), “Analysis of crack coalescence in rock-like materials containing three flaws-part II: Numerical approach”, *Int. J. Rock Mech. Min. Sci.*, **38**(7), 925-939.

Vallejo, L.E. (1987), “The influence of fissures in a stiff clay subjected to direct shear”, *Geotech.*, **37**(1), 69-82.

Vallejo, L.E. (1988), “The brittle and ductile behavior of clay samples containing a crack under mixed mode loading”, *Theoret. Appl. Fract. Mech.*, **10**(1), 73-78.

Vásárhelyi, B. and Bobet, A. (2000), “Modeling of crack initiation, propagation and coalescence in uniaxial compression”, *Rock Mech. Rock Eng.*, **33**(2), 119-139.

Vesga, L.F., Vallejo, L.E. and Lobo-Guerrero, S. (2008), “DEM analysis of the crack propagation in brittle clays under uniaxial compression tests”, *Int. J. Numer. Analy. Meth. Geomech.*, **32**(11), 1405-1415.

Wang, R., Zhao, Y., Chen, Y., Yan, H., Yin, Y.Q., Yao, C.Y. and Zhang, H. (1987), “Experimental and finite simulation of X-shear fractures from a crack in marble”, *Tectonophys.*, **144**, 141-150.

Wang, T., Dai, J.G. and Zheng, J.J. (2015), “Multi-angle truss model for predicting the shear deformation of RC beams with low span-effective depth ratios”, *Eng. Struct.*, **91**, 85-95.

Wang, X., Zhu, Z., Wang, M., Ying, P., Zhou, L. and Dong, Y. (2017), “Study of rock dynamic fracture toughness by using VB-SCSC specimens under medium-low speed impacts”, *Eng. Fract. Mech.*, **181**, 52-64.

Wong, L.N.Y. and Einstein, H.H. (2008a), “Crack coalescence in molded gypsum and Carrara marble: Part 1. Macroscopic observations and interpretation”, *Rock Mech. Rock Eng.*, **42**(3), 475-511.

Wong, L.N.Y. and Einstein, H.H. (2008b), “Crack coalescence in molded gypsum and Carrara marble: Part 2. Microscopic observations and interpretation”, *Rock Mech. Rock Eng.*, **42**(3), 513-545.

Wong, L.N.Y. and Einstein, H.H. (2009), “Systematic evaluation of cracking behavior in specimens containing single flaws under uniaxial compression”, *Int. J. Rock Mech. Min. Sci.*, **46**(2), 239-249.

Wong, R.H.C. and Chau, K.T. (1998), “Crack coalescence in a rock-like material containing two cracks”, *Int. J. Rock Mech. Min. Sci.*, **35**(2), 147-164.

Wong, R.H.C., Chau, K.T., Tang, C.A. and Lin, P. (2001), “Analysis of crack coalescence in rock-like materials containing three flaws-part I: Experimental approach”, *Int. J. Rock Mech. Min. Sci.*, **38**(7), 909-924.

Wong, R.H.C., Guo, Y.S.H., Liu, L.Q., Liu, P.X. and Ma, S.P. (2008), “Nucleation and growth of anti-wing crack from tips of strike-slip flaw”, *Proceedings of the 42nd US Rock Mechanics Symposium*, San Francisco, U.S.A.

Yang, S.Q. (2015), “An experimental study on fracture coalescence characteristics of brittle sandstone specimens combined various flaws”, *Geomech. Eng.*, **8**(4), 541-557.

Yoshihara, H. (2013), “Initiation and propagation fracture toughness of solid wood under the mixed mode I/II condition examined by mixed-mode bending test”, *Eng. Fract. Mech.*, **104**, 1-15.

Zeng, G., Yang, X., Yina, A. and Bai, F. (2014), “Simulation of damage evolution and crack propagation in three-point bending pre-cracked asphalt mixture beam”, *Constr. Build. Mater.*, **55**, 323-332.

Zhou, X.P. and Wang, Y.T. (2016), “Numerical simulation of crack propagation and coalescence in pre-cracked rock-like Brazilian disks using the non-ordinary state-based peridynamics”, *Int. J. Rock Mech. Min. Sci.*, **89**, 235-249.

Zhou, X.P. and Yang, H.Q. (2012), “Multiscale numerical modeling of propagation and coalescence of multiple cracks in rock masses”, *Int. J. Rock Mech. Min. Sci.*, **55**, 15-27.

Zhou, X.P., Gu, X.B. and Wang, Y.T. (2015), “Numerical simulations of propagation, bifurcation and coalescence of cracks in rocks”, *Int. J. Rock Mech. Min. Sci.*, **80**, 241-254.

Zhou, X.P., Bi, J. and Qian, Q.H. (2015), “Numerical simulation of crack growth and coalescence in rock-like materials containing multiple pre-existing flaws”, *Rock Mech. Rock Eng.*, **48**(3), 1097-1114.

CC